AFRL-AFOSR-UK-TR-2014-0018

Printable organic nanoelectronics for memory, sensors and display

ASIM RAY

BRUNEL UNIVERSITY
WOLFSON CENTRE FOR MATERIALS PROCESSING
KINGSTON LANE
UXBRIDGE UB8 3PH UNITED KINGDOM

EOARD Grant 13-3018

Report Date: February 2014

Final Report from 31 December 2012 to 30 December 2013

Air Force Research Laboratory
Air Force Office of Scientific Research
European Office of Aerospace Research and Development
Unit 4515 Box 14, APO AE 09421

REPORT DOCUMENTATION PAGE

Form Approved OMB No. 0704-0188

1. REPORT DATE *(DD-MM-YYYY)*	2. REPORT TYPE	3. DATES COVERED *(From – To)*
10-02-2014	Final Report	31 December 2012 – 30 December 2013

4. TITLE AND SUBTITLE

Printable organic nanoelectronics for memory, sensors and display

5a. CONTRACT NUMBER

FA8655-13-1-3018

5b. GRANT NUMBER

Grant 13-3018

5c. PROGRAM ELEMENT NUMBER

61102F

6. AUTHOR(S)

Asim Ray

5d. PROJECT NUMBER

5d. TASK NUMBER

5e. WORK UNIT NUMBER

7. PERFORMING ORGANIZATION NAME(S) AND ADDRESS(ES)

BRUNEL UNIVERSITY
WOLFSON CENTRE FOR MATERIALS PROCESSING
KINGSTON LANE
UXBRIDGE UB8 3PH UNITED KINGDOM

8. PERFORMING ORGANIZATION REPORT NUMBER

N/A

9. SPONSORING/MONITORING AGENCY NAME(S) AND ADDRESS(ES)

EOARD
Unit 4515
APO AE 09421-4515

10. SPONSOR/MONITOR'S ACRONYM(S)

AFRL/AFOSR/IOE (EOARD)

11. SPONSOR/MONITOR'S REPORT NUMBER(S)

AFRL-AFOSR-UK-TR-2014-0018

12. DISTRIBUTION/AVAILABILITY STATEMENT

Distribution A: Approved for public release; distribution is unlimited.

13. SUPPLEMENTARY NOTES

14. ABSTRACT

Two terminal memory devices have been successfully fabricated and evaluated using hybrid lead sulfide/metal free phthalocyanine nanocomposites and solution processed zinc oxide as active materials. For both cases, the size of the hysteresis and on-off ratios depend upon the bias scan rate, giving the best performance for the low scan rate. These memory devices have several advantages in terms of greater flexibility, low cost, easy fabrication procedure, 3-D stacking of memory layer and large area fabrication. Solution processable custom designed bisphthalocyanines have been employed in this project for the fabrication and integration of thin film organic devices on flexible substrates for displays. Ambipolar charge transport characteristics and On/Off ratio, low threshold voltage and contact resistances have been evaluated with a view to integrating into practical complimentary circuits. Voltammograms of specially designed lanthanide bisphthalocyanines exhibit one-electron quasi-reversible redox processes and these results are significant for the development of cost-effective, practical biosensors.

15. SUBJECT TERMS

EOARD, printable nanoelectronics, organic devices, self-assembly attachment, hybrid organic/inorganic quantum dots nanocomposites

16. SECURITY CLASSIFICATION OF:			17. LIMITATION OF ABSTRACT	18, NUMBER OF PAGES	19a. NAME OF RESPONSIBLE PERSON
a. REPORT	b. ABSTRACT	c. THIS PAGE			Kevin Bollino
UNCLAS	UNCLAS	UNCLAS	SAR	20	19b. TELEPHONE NUMBER *(Include area code)* +44 (0)1895 616163

FINAL REPORT

Printable organic nanoelectronics for memory, sensors and display

FA8655-13-1-3018

Academic Supervisor: Professor Asim K Ray

Wolfson Centre for Materials Processing

Brunel University Uxbridge,

Middlesex, UB8 3PH

Asim.ray@brunel.ac.uk

Project Supervisor: Dr. Ashwani K. Sharma

Space Vehicles Directorate Air Force Research Laboratory

3550 Aberdeen Avenue SE Kirtland AFB NM 87117

ashwani.sharma@kirtland.af.mil

TABLE OF CONTENTS

ABSTRACT

Two terminal memory devices have been successfully fabricated and evaluated using hybrid lead sulfide/metal free phthalocyanine nanocomposites and solution processed zinc oxide as active materials. For both cases, the size of the hysteresis and on-off ratios depend upon the bias scan rate, giving the best performance for the low scan rate.. These memory devices have several advantages in terms of greater flexibility, low cost, easy fabrication procedure, 3-D stacking of memory layer and large area fabrication. Solution processable custom designed bisphthalocyanines have been employed in this project for the fabrication and integration of thin film organic devices on flexible substrates for displays. Ambipolar charge transport characteristics and On/Off ratio, low threshold voltage and contact resistances have been evaluated with a view to integrating into practical complimentary circuits. Voltammograms of specially designed lanthanide bisphthalocyanines exhibit one-electron quasi-reversible redox processes and these results are significant for the development of cost-effective, practical biosensors.

LIST OF SYMBOLS USED

Symbols	Description	Page
Ag/AgCl	Silver/Silver chloride reference electrode	13
Au	Gold	8
C	Capacitance in equivalent circuit	8
CMOS	complementary metal oxide semiconductor	9
C_8PbPc	Octaoctyllphthalocyaninato lead phthalocyanine	7
DCM/TBAP	Dichloromethane/Tetrabutylammonium perchlorate	14
FESEM	Field Emission Scanning Electron Microscope	12
FTO	Fluorine-doped tin oxide	12
$I_{D(sat)}$	Saturation current	9
I_{sc}	Short circuit current	10
$LiClO_4$	Lithium perchlorate	14
NADH	reduced nicotinamide adenine dinucleotide	18
OTFT	Organic thin film transistors	11
PbS	Lead sulphide	6
QD	Quantum dots	6
R	Capacitance in equivalent circuit	9
$R_{16}GdPc_2$	1,4,8,11,15,18,22,25-octakis(octyl) gadolinium	9
$R_{16}LuPc_2$	bis[1,4,8,11,15,18,22,25-octakis(octyl)phthalocyaninato] lutetium(III)	14
V_a	Bias voltage applied between two electrodes in a planar configuration	9
V_G	Gate voltage	9
V_{oc}	Open circuit voltage	9
τ	Charging and discharging time constant	9
TOF	Time of flight	10
ZnO	Zinc oxide	13

FIGURE CAPTIONS

1.0 INTRODUCTION

Phthalocyanines (Pcs) which are macrocylic organic semiconductors have been studied for their role as an active layer in devices in light of their chemical and thermal stability, important optical absorption characteristics within the visible region and physically interesting optoelectronic properties Metallated and metal-free Pc derivatives substituted with hexyl (C_6H_{13}) and octyl (C_8H_{17}) chains at the 1,4,8,11,15,18,22,25- (non-peripheral) sites on the macrocyclic ring provide a particular set of compounds that are highly soluble in common organic solvents and have been demonstrated to exhibit spontaneous molecular alignment upon solvent evaporation to form molecular wire/cable type structures. Such behaviour promotes the development of reasonably non-discontinuous films over large areas. At elevated temperatures the compounds exhibit columnar liquid crystal behaviour. This range of properties renders this type of phthalocyanine compound potentially suitable for applications in printed plastic electronics.

2.0 TWO TERMINAL MEMORY DEVICES

Hybrid nanocomposites with inorganic lead sulfide (PbS) quantum dots (QDs) embedded in the matrix of metal free phthalocyanine analogues (Fgure 1(a), developed earlier was exploited in the present work for the design, fabrication and evaluation of two terminal memory devices.

(a)

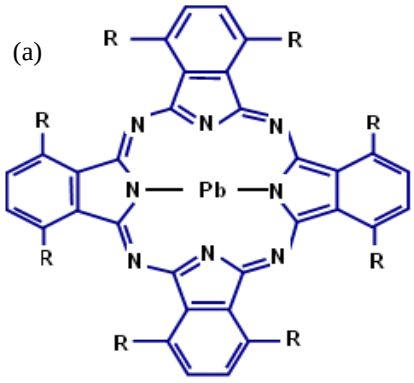

Compound**1** R= C_8H_{17}

(b)

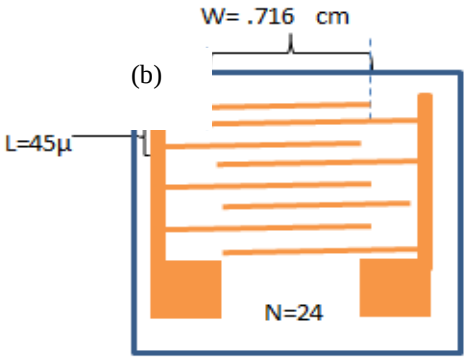

Figure1: Structural representation of 1-,4-,8-,11-,15-,18-,22-,25-octaoctyllphthalocyaninato lead (C_8PbPc) and (b) interdigitated gold (Au) electrodes on glass substrates

Figure 2(a) shows a set of reproducible room temperature current-voltage [$I(V_a)$] characteristics of H_2S treated C_8PbPc compound on the interdigitated gold electrode system when the applied voltage V_a was swept over the voltage range of ±50V at four different scan rates from $5mVs^{-1}$ to $5000mVs^{-1}$. In all cases, the direction of the current in the forward voltage sweep (0V → 50V and -50V →0V) is reversed in the backward sweep (0V ← 50V and -50V ← 0V), giving rise to the scan rate dependent hysteresis.

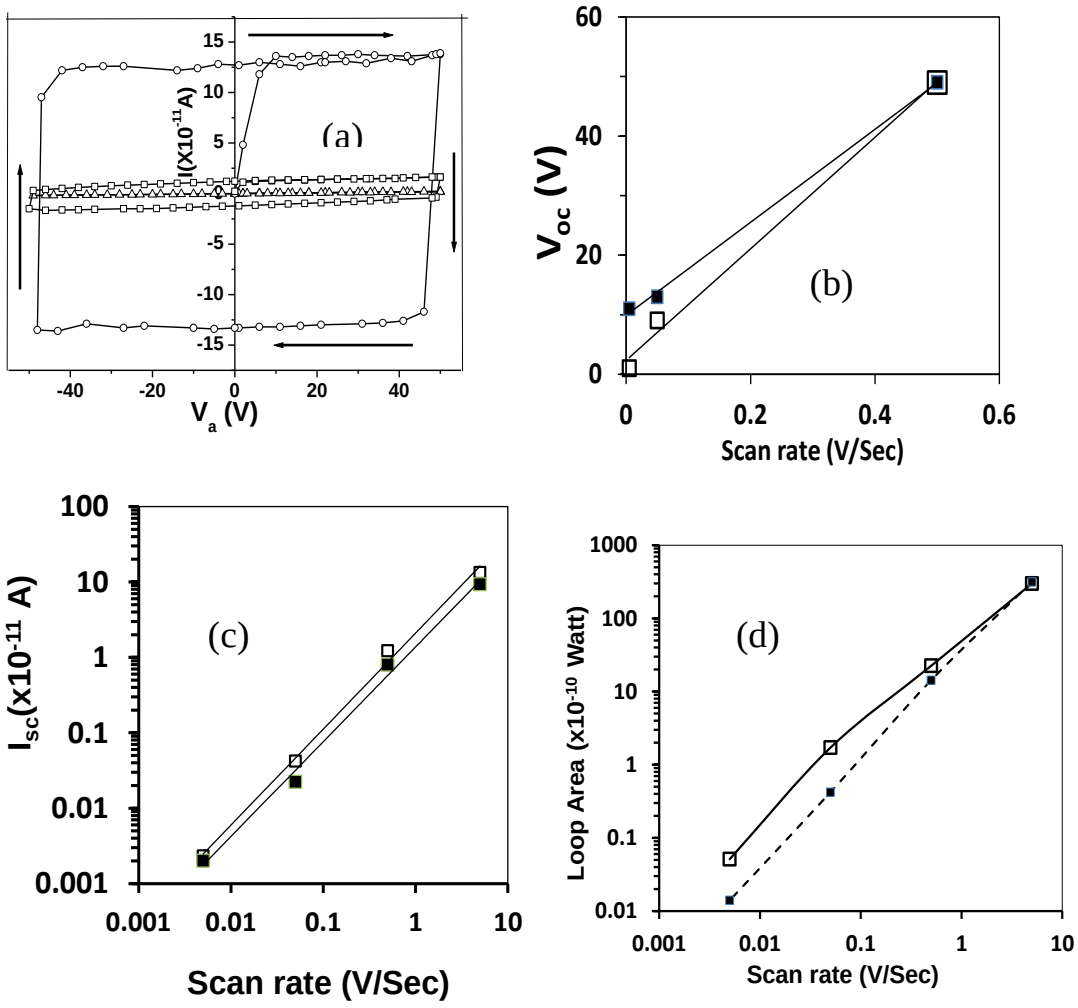

Figure 2: (a) Current vs applied voltage [$I(V_a)$] graphs of H_2S treated C_8PbPc compound as the applied voltage V_a is swept from OV to 50V in the forward and backward directions at the scan rate of $5mVs^{-1}$ (triangle), $500mVs^{-1}$ (square) and $5000mVs^{-1}$ (circle), arrows show the voltage sweep; Dependence of (b)

open voltage, (c) short circuit and (d) loop area for H_2S treated C_8PbPc compound (open squares) and metal free analogue compound (solid squares).

The effect of the scan rate on the planar charge transport in both films can be interpreted in an equivalent circuit model. The circuit consists of two passive electrical components, resistor R and capacitor C, connected in parallel. The net current I is the sum of the circulating current and displacement components in the form:

$$I = \frac{V_a}{R} + \frac{dV_a}{dt}\left[V_a \frac{dC}{dV_a} + \frac{\tau}{R}\right] \qquad (1)$$

where $\tau = CR$ is the charging and discharging time constant.

Figures 2(b), 2(c) and 2(d) show the dependence of the short circuit current I_{sc}, open circuit voltage V_{oc} and the hysteresis loop on the scan rate of the applied voltage V_a. The linear increase of I_{sc} with the scan rate $\left(\frac{dV_a}{dt}\right)$ for both samples is in keeping with the observation from Equation (1) that $I_{sc} = \frac{\tau}{R}\frac{dV_a}{dt}$ corresponding to $V_a = 0$. The open circuit voltage V_{oc} can be written as $V_{oc} = -\left[\frac{\frac{\tau}{R}\frac{dV_a}{dt}}{\frac{1}{R} + \frac{dV_a}{dt}\frac{dC}{dV_a}}\right]$ for $I = 0$. The gold forms an Ohmic contact with metal free phthalocyanine and the value of the capacitance C may thus be taken to be determined by the geometry, dimension and dielectric constant of the compounds, making $\frac{dC}{dV_a} = 0$. Therefore, the linear rise of V_{oc} with the scan rate in Figure 2(c) is also expected from Equation (1). . Values of time constant τ for H_2S treated C_8PbPc compound and metal free analogue are estimated to be 95s and 78s from the slopes of the graphs. The sweeping time decreases with the increasing scan rate and this time for the fast scan rates becomes shorter than the time constant τ. Under these circumstances, the majority of the carriers are swiftly swept from the injecting gold electrode finger to the counter electrode contributing largely to the circulating

current $\frac{V_a}{R}$. The trap-detraping mechanisms become progressively slow as the scan rate is increased.

3.0 THREE TERMINAL DEVICES FOR DISPLAY

The development of organic complementary metal oxide semiconductor (CMOS) like circuits and organic light-emitting transistors has stimulated the search for ambipolar organic semiconductors . The present investigation reports the results of time of flight (TOF) mobility measurements on drop-cast thin films of 1,4,8,11,15,18,22,25-octakis(octyl) gadolinium ($R_{16}GdPc_2$), Figure 3(a). Charge carriers are expected to be mobile along a rigid solid-like region consisting of closely packed molecules. Long-range mobilities have been measured in the present investigation on 5μm thick films on the microsecond timescale for the field varying from $2.25\times10^4 Vcm^{-1}$ to $11.2\times10^4 Vcm^{-1}$ The TOF mobility which is characteristic of bulk samples becomes, therefore, relevant to real applications.

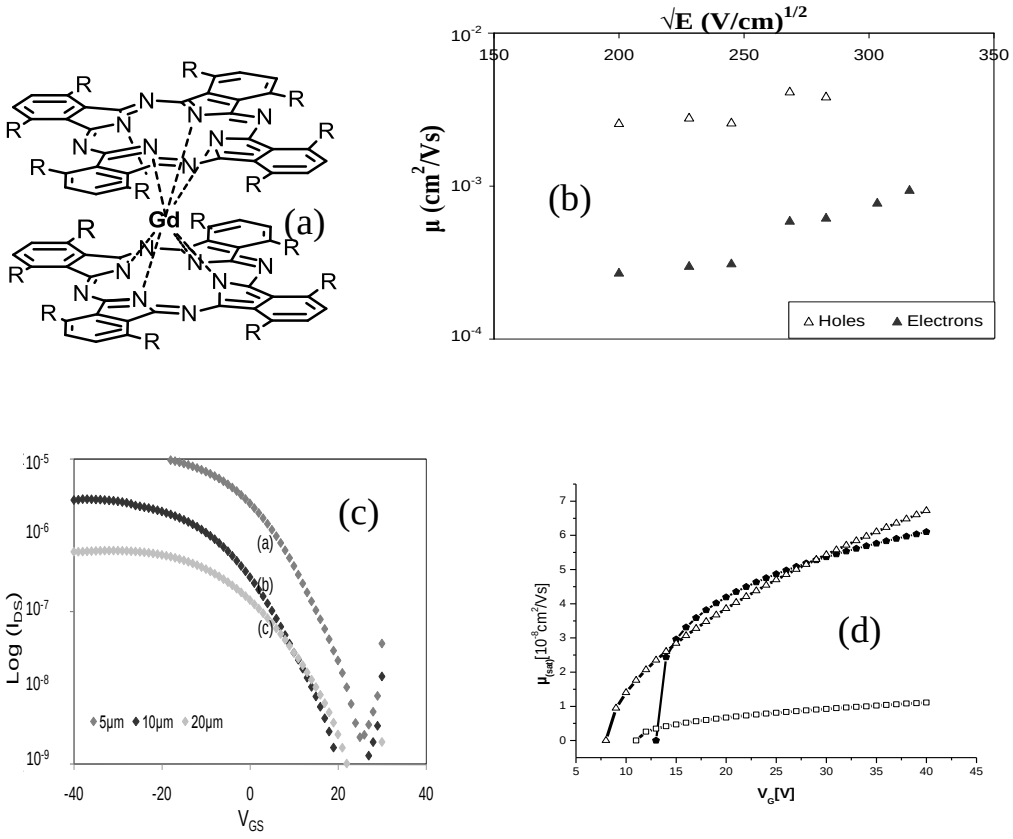

Figure 3: (a) Chemical structure of $R_{16}GdPc_2$, where R corresponds to a C_8H_{17} (octyl) chain, (b) Poole-Frenkel plots for hole (circles), electron (square) and electrons after sample degradation

(triangle) mobilities in $R_{16}GdPc_2$, calculated, parametric in electric field (c) transfer characteristics and (d) (Open triangle 20μm, solid pentagon 5μm and open star 10μm)

Values of both electron and hole carrier mobilities can be individually determined in a single experiment by changing the polarity of the applied bias voltage. The TOF technique is thus capable of distinguishing between traps for electrons and holes in the same sample. Values of field electron mobility are found to vary betwwen $0.91\times10^{-4}cm^2V^{-1}s^{-1}$ and $1.3\times10^{-4}cm^2V^{-1}s^{-1}$. Values of $1.2\times10^{-2}cm^2V^{-1}s^{-1}$ and 1.0×10^{-24} $cm^2V^{-1}s^{-1}$ were determined for hole mobilities. Pre-patterned bottom gate/bottom contact organic field effect transistors (OFETs) with highly doped silicon wafers as the gate electrode and thermally grown (200 nm) silicon dioxide as the gate dielectric. The channel width remained unchanged at 10mm but different channel lengths, 5μm, 10μm and 20μm, respectively, were investigated for the same $R_{16}GdPc_2$ active layer. The current modulation (on/off current ratio) was found to be 10^2 from the transfer characteristic in Figure 3 (c) of source todrain I_{SD} versus gate voltage V_{GS} for drain voltage of $-40V$ independent of the channel length. The charge carriers induced by the gate voltage in the channel became captured by the traps, the existence of which are inherent with the polycrystalline morphology of the $R_{16}GdPc_2$ film. The mobility of the carriers is therefore dependent upon the gate voltage in a power law form as shown in 3(d). Values of 2.88×10^{-7} cm^2/ Vs, 9.36×10^{-6} cm^2/ Vs and 1.93×10^{-6} cm^2/ Vs for saturation mobilties for 5μm, 10μm and 20μm, respectively. For hole conduction, the 20μm long channel OFETs was found to switch on the lowest voltage of about 8V while the smallest threshold voltage was observed for 9.2V for 10μm. The shortest channel lengths have produced the highest value of the threshold voltage Finally the active phthalocyanine layer is found to have formed Schottky type contacts with both source and drain electrodes. Therefore, the carrier movement in the bottom contact OTFT contact is mainly influenced by the contact resistances at the source and the drain contacts, respectively. The contact resistance is found to increase with the channel length from $3.6\times10^7\Omega$ to $1.8\times10^8\Omega$ corresonding to 5μm and 20μm long channels for the hole conduction. Similar observations have been made for electron transport.

4.0 LOW COST ZINC OXIDE FOR MEMRISTORS

Thin-film zinc oxide (ZnO) continues to attract attention because of its low toxicity and its many applications in solar cell technology and as thin-film gas sensors, varistors, and a phosphor for color displays. A variety of methods have been reported for the preparation of ZnO thin films. For example, films have been deposited by thermal evaporation, rf-sputtering, chemical vapor deposition, laser ablation, and variations on these methods. In addition to these techniques, spray pyrolysis has received fair amount of attention because of its simplicity and consequent economics as it does not require a high vacuum apparatus. In this work, Zinc oxide was spin-coated onto fluorine-doped tin oxide (FTO) coated glass slides (TEK 15, Pilkington UK) with surface resistivities of ~15Ω/square.

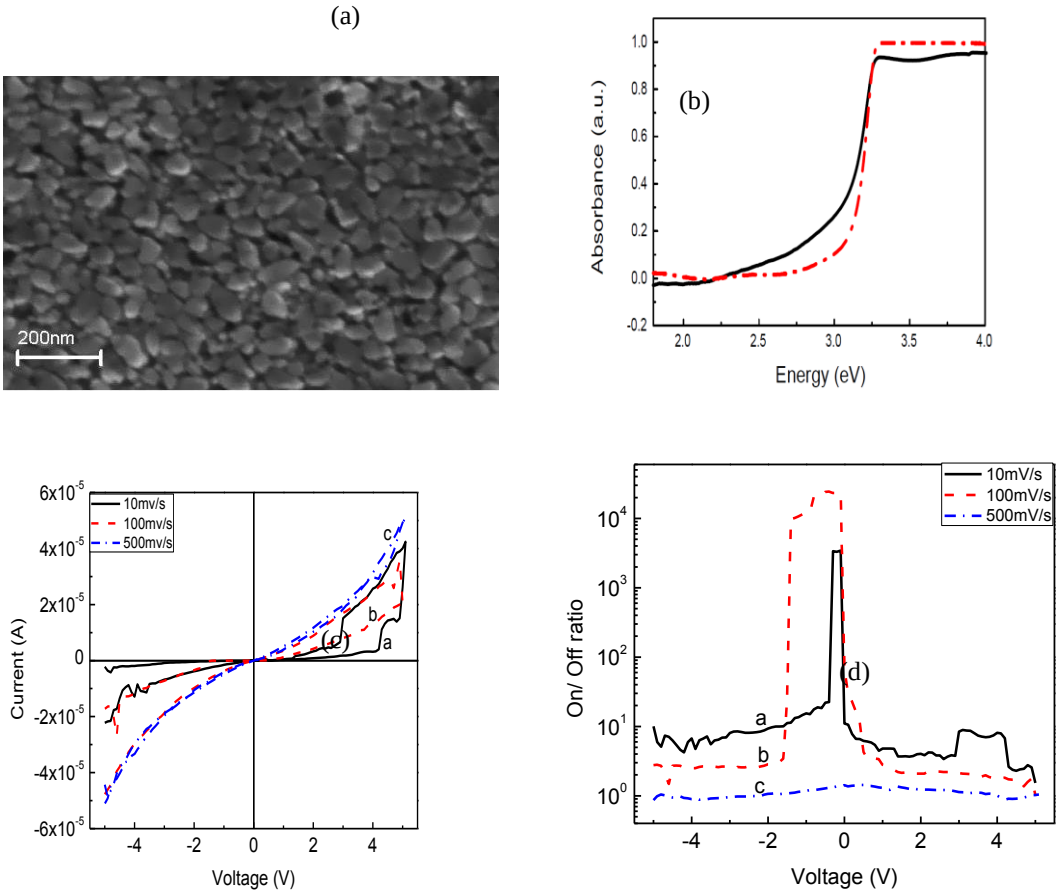

Figure 4. **(a)** FESEM Image of the ZnO coating., (b) UV-visible transmission spectra of as deposited (broken line) and annealed (solid line) ZnO films on silica slides, (c) current-voltage characteristics for -5V to 5V (1st cycle) at the scan rate of (a) 10mV/s (solid line) (b) 100mV/s (broken) and (c) 500mv/s (broken lines with dots) and (d) On /off ratio vs voltage at different scan rate for annealed ZnO film from -5V to 5V (1st cycle) for the scan rate of (a) 10mV/s (solid line), (b) 100mV/s (dash line) and (c) 500mV/s (dash dot line).

The morphology of the ZnO deposits was examined using a Field Emission Scanning Electron Microscope (FESEM). Figure 4(a) shows a FESEM micrograph of the as-deposited coating. The particles were not perfectly spherical, but had a more irregular morphology, with flat surfaces typical of crystalline materials. The packaging density of the deposit is very good for a deposit such as this. UV/vis absorbance spectrum in Figure 4 (b) shows two distinct regions: (i) sharp absorption edge due to interband transition in the incident photon energy hν range between 3.15-3.25eV and (ii) absorption tail at the low photon energies in the range of 2.20eV and 2.32eV representing the localized states tailing into the band gap . Using the Tauc plots, the transition is found to be direct for both samples and values of 3.15eV and 3.12eV are estimated for the direct optical band gap of as-deposited and annealed films, respectively. A Keithley 617 electrometer was employed for current voltage measurements on spin-coated ZnO films onto the FTO substrate in high vacuum ($\leq 10^{-4}$mbar) at room temperature for the voltage range ±5V. Before coating a channel was removed in the FTO layer by light mechanical abrasion so as to define two areas on each slide which were electrically isolated from each other. The slides were then repeatedly washed in acetone to remove any surface contamination. .Figure 4(c) presents current-voltage characteristics obtained at different scan rates. of Au/ZnO/FTO sandwich structure shows typical bipolar resistive switching behaviour under the steady voltage sweep from -5V to 5V in one complete cycle. The voltage was applied to the bottom electrode while the top electrode remained grounded. During the sweep measurement, the voltage was swept from -5V to +5V then returning from +5V to -5V with different sweeping steps. The characteristic curves of this structure exhibit a symmetric non linear characteristic when voltage sweeping step is 500mV/s. Multiple resistive state of the structure is revealed when it is swept at 10mv/s and 100mV/s. The on /off ratio i.e., ratio of currents obtained at same voltage for two different conducting state has been plotted against voltage for three different voltage sweeping step in Figure 4(c). It is observed that on/off ratio at -0.1V are 1.34 for 500mV/s, 2.2×10^4 for 100mV/s and 3.4×10^3 for 10mV. High on/off ratio (> 1000) is obtained using low reading voltage (e.g. -0.1V) for curve under 100mV/s sweeping step. Two conducting state behaviours can be explained by creation of oxygen vacancies within ZnO layer. Oxygen vacancies were gradually created by removing oxygen ions from the substantial sites in ZnO layer which form conducting and non-conducting layers inducing memristor

behaviour. There was no significant degradation of current value of the device when it was measured after one month indicating its good stability and reproducibility.

5.0 CYCLOVOLTAMETRIC STUDY FOR BIOSENSENING

Cyclic voltammetric measurements on the bis[1,4,8,11,15,18,22,25-octakis(octyl)phthalocyaninato] lutetium(III) ($R_{16}LuPc_2$) molecules (Figure 5(a)) in the solution, the Ag/AgCl reference electrode was enclosed in a Luggin capillary, filled with the DCM/TBAP mixture. The capillary tip was placed close to the platinum working electrode with a view to minimising the undesirable electrical resistance. The platinum wire counter electrode remained immersed in the Dichloromethane/Tetrabutylammonium (DCM/TBAP) perchlorate solution. The voltage was swept between ±2.5 V at 100 mV/sec scan rate. Redox reaction activities were also examined on homogeneous thin films of $R_{16}LuPc_2$ deposited on indium-tin-oxide (ITO) coated glass substrates as a working electrode of a three-electrode GiIIAC potentiostat. A high purity platinum wire counter electrode and an Ag/AgCl reference electrode were used in a three-electrode configuration with a working electrode. The steady state cyclic voltammogram curves were recorded at room temperature in an aqueous medium of 1.5M $LiClO_4$ (pH = 7.2) by potentiodynamic sweep between 0V and 1.5V with a rate of 100mV/sec with respect to the reference electrode. An oxygen free environment was maintained by the constant flow of pure N_2 gas during the voltammetric experiments.

Figure 5(b) shows a typically reproducible cyclic voltammogram of the $R_{16}LuPc_2$ molecules in the solution phase, displaying the presence of two anodic potential peaks E_{pa} at +1.54V and -0.40V and two cathodic potential peaks at +0.365mV and -1.26V in the voltage sweep between ±2.5V. These lead to the formation of monovalent cations and anions respectively and can be represented in the form:

$$R_{16}LuPc_2^- \underset{+e^-}{\overset{-e^-}{\rightleftharpoons}} R_{16}LuPc_2 \underset{+e^-}{\overset{-e^-}{\rightleftharpoons}} R_{16}LuPc_2^+$$

Values of the formal potential (E_0) and the peak potential separation ΔE for are estimated to be 0.95V and 1.175V for oxidation from the knowledge that $E_0 = (E_{pa} + E_{pc})/2$ and $\Delta E = (E_{pa} - E_{pc})$. Using the same relations, E_0 = -0.81V and ΔE = 0.86V were obtained for reduction process. The difference between the formal potentials for oxidation and reduction is found to be 1.76V. This value corresponds well to the HOMO–LUMO gap of the molecule.

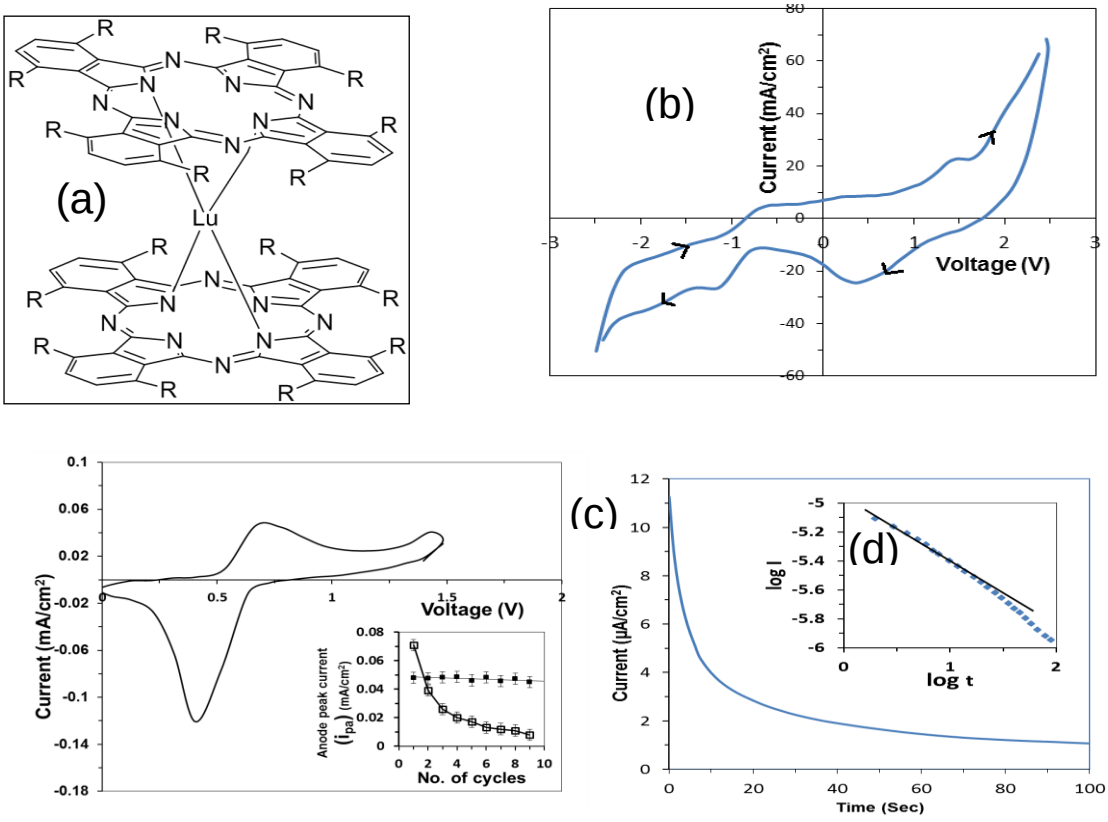

Figure5: (a) Bis[1,4,8,11,15,18,22,25-octakis(octyl)phthalocyaninato] lutetium(III) [$R_{16}LuPc_2$ R = C_8H_{17} (octyl) chains], (b) Cyclic voltammogram of 0.33 M $R_{16}LuPc_2$ in DCM solvent with 0.1 M TBAP at 25 °C. Scan rate 100mV/sec. (c) Cyclic voltammogram of $R_{16}LuPc_2$ spun film on ITO electrode in a 1.5 M LiClO4 aqueous solution at 25 °C. Scan rate 100mV/sec. Inset, dependence of the anodic peak current obtained in an aqueous solution of 1.5 M $LiClO_4$ (solid squares) and 1 M KCl (open squares) on number of cycles and (d) Current density time transients at applied oxidising potential 0.88 V for 20 minutes in 1.5 M $LiClO_4$. (Inset) (Inset) logarithmic plots of Current density vs time at same applied potential.

A single pair of the peak anodic cathodic potentials was observed in the voltammogram in Figure 5(c) for spin coated films of $R_{16}LuPc_2$ molecules for voltage sweep between 0V and 1.5V. As the voltage was increased from 0V to1.5V, the film became progressively oxidised, displaying the anodic peak currents (i_{pa}) of 0.046 $mAcm^{-2}$ at the peak anodic potential E_{pa} = 0.70V vs the reference electrode. The cathodic (i_{pc}) peak current of 0.12 $mAcm^{-2}$ was observed at the cathodic potential E_{pc} = 0.41 V, giving rise to the reduction of the film in the reverse sweep. Values of the formal potential (E_0) and the peak potential separation ΔE are estimated to be 0.56V and 0.29V.

The characteristic value of ΔE = 59mV for one electron reversible process is much smaller than those obtained for the $R_{16}LuPc_2$ molecules in both solution and solid phases. The large values of ΔE may be attributed to due to the effect of substitution of octyl ($-C_8H_{17}$) chains at non-peripherial positions of the $R_{16}LuPc_2$ molecules. This observation is also supported by the earlier work on similarly non-peripherally substituted octa-alkylated metal-free phthalocyanine molecules. Values of ΔE became greater with increasing length of substituted alkyl chains length leading to the diminished degree of reversibility. The effect of the substitution on the formal potential E_0 is also reported. For example, E_0 = 0.78V was observed for the drop cast film of the double-decker lutetium(III) phthalocyanine molecules, substituted with dodecyl ($-C_{12}H_{25}$) on each ring.

The ratio of the anodic (i_{pa}) to cathodic (i_{pc}) peak currents is estimated to be 0.35, implying that only about one third of neutral $R_{16}LuPc_2$ on the forward sweep become reoxidised to $R_{16}LuPc_2^+$ on the reverse sweep. The electron transfer is, therefore, a quasi-reversible process which is not completely in electrochemical nature but is expected to have involved other physical or chemical processes. Values of $2.20\times10^{-3}cms^{-1}$, 1.0×10^{-5} $cm^2s^{-1}$and 0.5 were deduced for the heterogeneous electron transfer rate constant, diffusion coefficient and charge transfer coefficient respectively from the numerical solution of the Tafel equation for the forward sweep.

As the overall reaction equilibrium depends upon the ion transfer energetics, the choice of the electrolytes is important for an observable electron transfer in the polarization domain. Cyclic voltammetric measurements were repeated using 1 M aqueous KCl (pH = 7.0) as electrolyte in order to determine the electrolyte dependent stability of the working electrode. Ion exchange reactions between the electrolyte ions and the ions in the

aqueous phase can alter the starting conditions for the electron transfer reaction. As shown in the inset, the anodic peak current i_{pa} decreased with the number of cycles up to 10 cycles. Similar instability was also observed in voltammograms of an electrophoretically deposited film of a different lutetium bisphthalocyanine derivative. It shows that the KCl electrolyte counter anions became less active in forming the counterion on the singly oxidized form of $R_{16}LuPc_2^+$ possibly due to penetration of KCl into the film. This ion-pairing effect caused the degradation of anodic peak current i_{pa} with the voltage cycling. However, the peak current remained largely stable for the 1.5 M $LiClO_4$ electrolyte solution indicating invariant nature of ion-paring with supporting electrolyte anions.

The current-time transient curves were recorded under the application of a constant oxidising potential of 0.88V. As shown in Figure 5(d), a sharp spike to current density of 11μA/cm^2 was observed at the start. The plot in the inset of the current density against the time on logarithmic scales is linear over the time less than 60sec, giving a value of 0.53 for the slope. This implies the validity of the Cottrell law. The oxidation of the $R_{16}LuPc_2$ thin film was found to be complete within the period of 60sec, which is due to the accumulation ClO_4^- near the working electrode. After this time, the rate of diffusion of the ions to the interface between the $R_{16}LuPc_2$ film and the electrolyte was much slower than that of the oxidation process, giving rise to the rapid drop of current.

6.0 SCOPE OF EXPLOITATION AND APPLICATIONS

The past three decades have seen intense research efforts and activities in the development of plastic electronics for potential exploitation in organic integrated circuits, applications of which include radio frequency identification tags, organic thin-film transistor (OTFT) arrays for active matrix displays and flexible sensors for wearable and implantable devices. Non-peripherally substituted octahexyl bisphthalocyanine in its stable polymorphic phase exhibits intrinsic ambipolar transport at a low electric field of 10^4 V/cm. The long term environmental stability of the organic semiconductor is a major concern. Oxygen has a high electron affinity and may diffuse from the surface into the bulk. These diffused oxygen molecules may possibly act as deep level trapping centres of electrons. Low degradation of the phthalocyanine without any encapsulation is very

promising for realising single-material complementary field effect transistor based circuits with lower-power dissipation and good noise margin. Cost-effective solution processing is also compatible for exploitation.

The quasi-reversible one-electron redox processes in non-perpheral octaoctyl substituted lutetium bisphthalocyanine ($R_{16}LuPc_2$) molecules are believed from the cyclic voltammetry studies to be independent of the lutetium central ion but associated with ring-based processes during oxidation and reduction. The electrochromic behaviour of the film was examined by cyclic voltammetry establishing the value of 0.88V for bias potential for oxidation. The realisation of reduced nicotinamide adenine dinucleotide (NADH) biosensing probes is currently attracting considerable attention for monitoring mitochondrial function as an electron exchanger. Oxyradicals which are also produced from NAD^+ to NADH redox reactions are detrimental to brain proteins, causing age-related diseases like Alzheimer's and Parkinson's diseases. NADH sensors have also been identified for possible use for determining the training efficiency of athletes, diagnosis of cortical spreading depression and monitoring jet-lag induced fatigue. The complete recovery of the oxidised bispthalocyanine film to its neutral form via NADH reduction leads to the realisation of reusable membranes to be incorporated in practical biosensors for the point care uses. The $R_{16}LuPc_2$ film remains sensitive at least for three months even when left in open space. However the reduction rate is slow but further work is required to develop well-designed calibration protocols.

PROJECT STUDENTS:

Mrs Chandana Pal MSc is registered with Brunel University for PhD degree in Materials Engineering as of 2011. The title of the project is 'Study of Optical and Electrical Properties of Novel Substituted Phthalocyanine molecules in Thin Film Formulations.

The experimental investigation of interaction between lanthanide phthalocyanine derivatives with redox biomolecules like NADH (nicotinamide adenine dinucleotide phosphate) and vitamin C will be undertaken in term of optical absorption and voltammetric process. Phthaiocyanine is a macrocyclic compound that is widely used in dyeing, gas sensors, biosensors, photography and laser printing. NADH is important

cofactor in metabolism and Vitamin C is an antioxidant. Determination of concentration of these cofactors is relevant to diagnosis of diseases. She will be submitting her thesis on thin films of non-periherally octyl substituted liquid crystalline phthalocyanines in February 2014.

Miss Tsegie Mariam Faris B Eng is registered with Brunel University for M Phil degree in Materials Engineering as of 2011 on the project of "Modelling of Phthalocyanine based thin film organic transistors". Experimental data on output and transfer characteristics were obtained for tetrasubstituted zinc phthalocyanine ($ZnPc_4$) organic thin film transistors. Physical models have been developed to examine the effects of grain boundary, traps in the interface between gate and semiconducting layers and the contact resistances in the source and drain.

ACKNOWLEDGEMENTS

Sincere gratitude is due to Lt Col Kevın Bollıno, Program Manager at the European Office of Aerospace Research and Development, London office for his support. Support from EOARD is acknowledged in all publications.

PUBLICATIONS

1. Pal C, SharmaA.K., Cammidge A.N., Cook M. J, Ray, A.K 2013 **Octaoctyl Substituted Lutetium Bisphthalocyanine For NADH Biosensing.** *J. Phys. Chem. B* 117(48 **):** 15033-15040 **DOI:** 10.1021/jp4078568. .
2. Pal C., Ojeda J. J.,. Cook M. J, Sharma A. K, and Ray, A.K. 2013 **Novel Liquid Crystalline Gadolinium Bisphthalocyanine Derivatives in Two Terminal Electronic Device.** 11th International Conference on Materials Chemistry (MC11) 08-JUL-2013 to 11-JUL-2013.
3. Harris P., Paul S., Pal C., Sharma A. K. and Ray, A.K.2013 **Charge Transport in solution processed thin films of Zinc Oxide.** The 25th International Conference on Amorphous and Nano-crystalline Semiconductors August 18–23, 2013 Toronto, Ontario Canada.
4. Faris T., Basova T., Chaure N. B., Sharma A. K, Durmuş M., and Ray, A.K. **Effects of annealing on device parameters of organic field effect transistors using liquid crystalline tetrasubstituted zinc phthalocyanine.** EuroPhysical Letters (under review)